Hindawi
Advances in Materials Science and Engineering
Volume 2022, Article ID 3104199, 9 pages
https://doi.org/10.1155/2022/3104199

Research Article

The Influence of Process Parameters on the Mechanical Properties of Friction Stir-Welded Dissimilar Aluminium Alloys AA2219 and AA7068

Mohamad Reda A. Refaai,[1] **R. Meenakshi Reddy**,[2] **A. Radha**,[3] **and David Christopher**[4]

[1]*Department of Mechanical Engineering, College of Engineering, Prince Sattam Bin Abdulaziz University, Alkharj 16273, Saudi Arabia*
[2]*Department of Mechanical Engineering, G. Pulla Reddy Engineering College, Kurnool 518007, Andhra Pradesh, India*
[3]*Department of Mechanical Engineering, Loyola-ICAM College of Engineering and Technology, Chennai, Tamil Nadu 600034, India*
[4]*Department of Mechanical Engineering, College of Engineering, Wolaita Sodo University, Sodo, Ethiopia*

Correspondence should be addressed to Mohamad Reda A. Refaai; m.rifaee@psau.edu.sa

Received 17 December 2021; Accepted 4 February 2022; Published 29 March 2022

Academic Editor: P Ganeshan

A practical solution is friction stir welding (FSW) of heterogeneous alloys in industrial applications. The welded joint's mechanical strength has been improved by combining two different alloys (AA2219 and AA7068). The focus of this study was on friction stir-welded heterogeneous metals' microhardness and material properties. It is possible to work with either hot or cold aluminium alloy, as it is heat treatable. Revitalizing and precipitation hardening follow the heat treatment. The welded joints' hardness was assessed in several locations. Different joints' tensile characteristics are compared. According to the stress-strain curve, the FSW settings' mechanical properties were spread throughout the material flow. In terms of tool profiles, the cylindrical threaded profile is critical. One-third of the efficiency is due to it. A 195 MPa strength was reached in the cylindrical threaded pin profiled tool. In a new study, researchers discovered that cylindrical threads have faster rotary motion, transversal, and D/d speeds. The cylindrical threaded tool provided the highest tensile strength and was superior to other materials. This phase of the material characterization included measurements of tensile strength and hardness.

1. Introduction

Friction stir welding (FSW) was developed in 1991 by the Welding Institute (TWI) in the United Kingdom as a solid-state fusion process. FSW is a cutting-edge technology for permanently connecting materials. FSW involves rotating and gently plunging a cylindrical, shouldered tool with a profiled probe into the joint line between two pieces of sheet or plate material that are butted together. The pieces are held together throughout the welding process to prevent the abutting joint faces from being driven apart [1]. In a wide range of industrial applications, aluminium alloys (AA2219-AA7068) are widely used: for aircraft structures, for maritime applications such as ships and pipelines, for automobiles and shipbuilding, and so on. Due to car body shells' lightweight structures, there are more design requirements than ever before [2, 3]. The wrought aluminium-copper alloy AA2219 belongs to the family of (2000 or 2xxx series). Heat treatment may create tempers with greater strength but poorer ductility. AA7068 alloy is a heat treatable wrought alloy with excellent thermal conductivity, strong fatigue strength, and excellent anodizing reaction. The FSW process is a one-of-a-kind approach to developing lightweight alloy structures. Avoiding manufacturing faults such as approximation permeability, sludge, dispersion, liquid cracks, and heat affected zones (HAZ) is achievable. It is like saying that various alloys of joint technology are used in fabrication because fusion welding has melted numerous

alloys of joint technology while developing secondary phase owing to thermal absences employing base materials as a pin device [4]. It is because of this that the temperature distribution in nugget zones (NZs) has increased more slowly when compared to alloys of different compositions. Collecting rotational and transverse speeds is the ideal approach to this problem. As a result, the instrument is critical in FSW [5]. Using a stirring motion, this tool profile or form is effective at transferring the substance from the base material. Tool profile and various process parameters are not the only factors affecting FSW behaviour [6]. Figure 1 shows an FSW's schematic diagram.

The optical microscope has been used by FSW to identify the four functional zones, including the parent material (PM), NZ, the thermally mechanically impacted zone (TMAZ), and the HAZ. The movement of materials along the route of the welding process generates all of these zones [7, 8]. Plastic deformation has increased on work piece's top surface due to heat generated by rubbing tool. Material flow behaviour refers to the swept volume to pin volume ratio. For a given condition, the swirl revolves at the rotational and transverse speeds specified [9].

In previous studies, AA 2219 and AA 7068 in FSW were extensively examined. Different FSW joints and mechanical characteristics evaluations no longer include quick microstructural investigations [10]. Scientists carried out tensile and microhardness tests on various alloys and used optical microscopy to evaluate FSW elements of the process based on the microstructure of welded joints as part of this investigation [11–18]. This approach's design principles have been described in FSW using multiple tool profiles to combine various alloys. AA 2219 tool profile faults have been analysed and tested which may be found throughout the specification [14]. The interplay between the tool pin profile rotation speed and the heat plastic behaviour on the plate surface caused the heat plasticity [15, 16]. FSW will greatly benefit from this information. It has been determined that process parameter effects on weld zone hardness have been investigated by conducting a hardness survey there. We learned a lot about the connection between microstructure and mechanical properties [17–19].

2. Tool Design

The FSW method includes tool design in some capacity. It examines the properties of the two types of wrought aluminium alloys and compares them. This welder's tool should have dimensions such as height, depth, pin diameter, and width at the shoulder. The FSW technique relies heavily on the pin and shoulder components [20, 21]. The FSW pin forms such as direct cylindrical, taper threaded, and cylindrical have been investigated in this work. FSW pin shapes include the advancing and retracting sides of the rotating pins used to mix the ingredients. To connect the materials, a material deformation will be caused by this pin. The mechanical characteristics and flow characterization were investigated using a variety of tools. During the FSW process, the tool came in with a variety of shapes and sizes, with temperature dispersion as a heat transfer mechanism

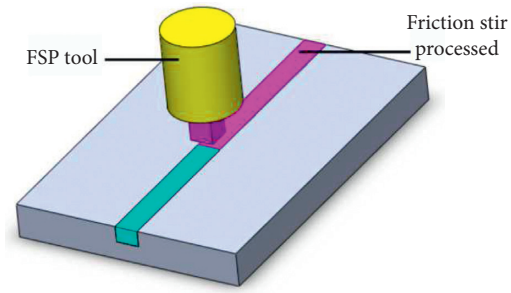

Figure 1: Friction stir welding.

for mixing incompatible alloys. A tool used to spin and add material flow characteristics to the power is sent through it. Tool requirements include things like how much torque is exerted at the pin's end. It would be possible to assess the claimed torque as traction force. Among the welding materials, the temperature normally lived within a specified range is one of the ideal tool parameters' shoulder with heat transmission and flow behaviour. As a flow model, the impact of the tool's shoulder was investigated. We looked at a temperature distribution and material deformation with this thermocouple as part of our FSW process research [22]. The varied tool sizes can adjust the FSW grain size zones. As seen in Figure 2, these tool-end surfaces have a wide range of shapes, including knurling, squared, threaded, scrolls, and ridges.

Certain characteristics, such as product flow behaviour and adequate mechanical toughness under various stress circumstances, should be present on the tool pin surfaces. It is possible that, between an increased shear creation and distortion, there is shoulder and base material which can indicate consistent mixing of incompatible alloys in the material. The probe area mostly controls the material's deformation depth. In terms of maintaining the metals' flow behaviour as well as the various tool pin performance, this is necessary. This is crucial. It compresses the weld centre lines together. The convexity of the material aided a stirring motion known as NZs. The surface probe's primary purpose is to withstand the enormous forces generated while plunging. A very sophisticated and very diverse tool with each movement of material is around the probe.

3. Experimental Setup

FSW was collected in a technical arrangement, as shown in Figure 3. This study looked at the different specimens AA 2219, magnesium, and silicon. AA 2219 is on the leading edge, while AA 7068 is on the reversing edge. The high material flow stability and strong resistance capacity of these AA 2219 alloys make them superior to other materials in terms of design requirements. This FSW method made use of both plates ($120 \times 120 \times 6$). Tables 1 and 2 analyses the AA 2219 and AA7068 alloys' chemical and mechanical properties. To combine dissimilar alloys with different optimal constraints, such as rotatory speed, transversal speed, and different load circumstances, the trail experiments were finished up to this point. Using a vertical milling machine,

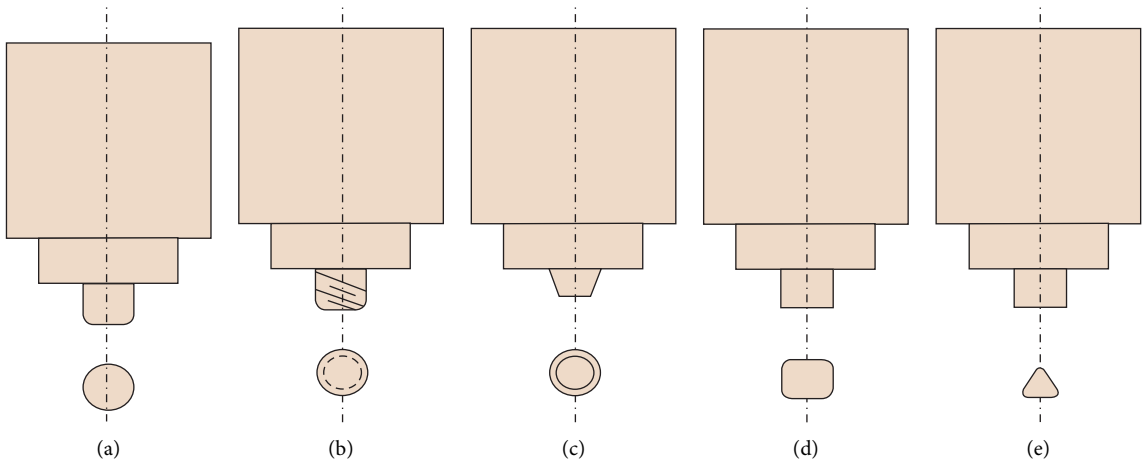

Figure 2: Different tool profiles: (a) straight cylindrical, (b) threaded cylindrical, (c) tapered cylindrical, (d) square, and (e) triangle.

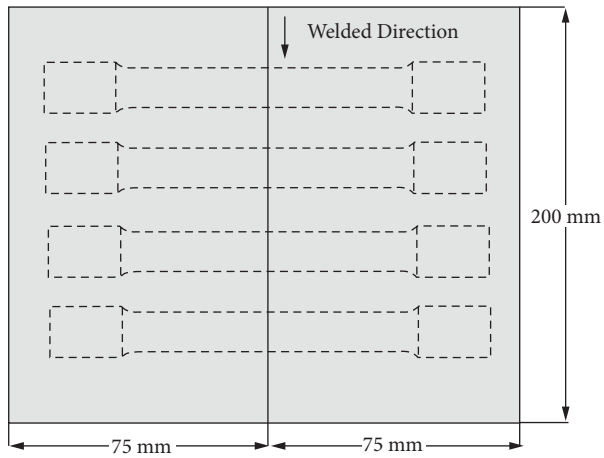

Figure 3: Specimens for tensile testing in the FSW joints.

Table 1: Dissimilar alloys' chemical composition.

Element	Mg	Ni	Si	Fe	Cu	Ti	Al
AA2219-T6	1.60	1.0	0.18	1.1	2.30	0.07	93.7
AA7068-T6	2.7	0.12	5.1	0.35	2.0	0.58	88.1

Table 2: Dissimilar alloys' mechanical composition.

Element	Yield strength (MPa)	Tensile strength (MPa)	Elongation (%)
AA2219-T6	335	363	21
AA7068-T6	495	589	16

FSW is applied. Different pin profiles have the same process limit functions. Pin diameter is 6 millimetres, shoulder diameter and tool pin height are both 18 millimetres, and plate thickness is 6 millimetres. The heat conductivity and resistivity of this tool pin are excellent. The welded plate has a tool pin in the middle of it. Factors of the system such rotating speed, cross-speed, and load capacity were tested on a total of nine samples. Table 3 lists the weld conditions and process parameters.

The UTM machine tested is used for tensile strength. As a welded work piece, precipitated dissimilar alloys are hardened by applying load in the transverse direction. Tensile tests were performed on nine different samples to get the optimal average value.

The nugget region was subjected to a Vickers hardness test as part of the welded zones' transverse load portion. This area has been designated as a TMAZ by the government. The following sections have analysed or plotted the hardness

Table 3: Friction stir-welding criteria.

S. no	Rotatory speed (rpm)	Transformational speed (mm/min)	Pin description
1	900	40	Cylindrical
2	1100	80	Threaded cylindrical
3	1300	120	Taper threaded

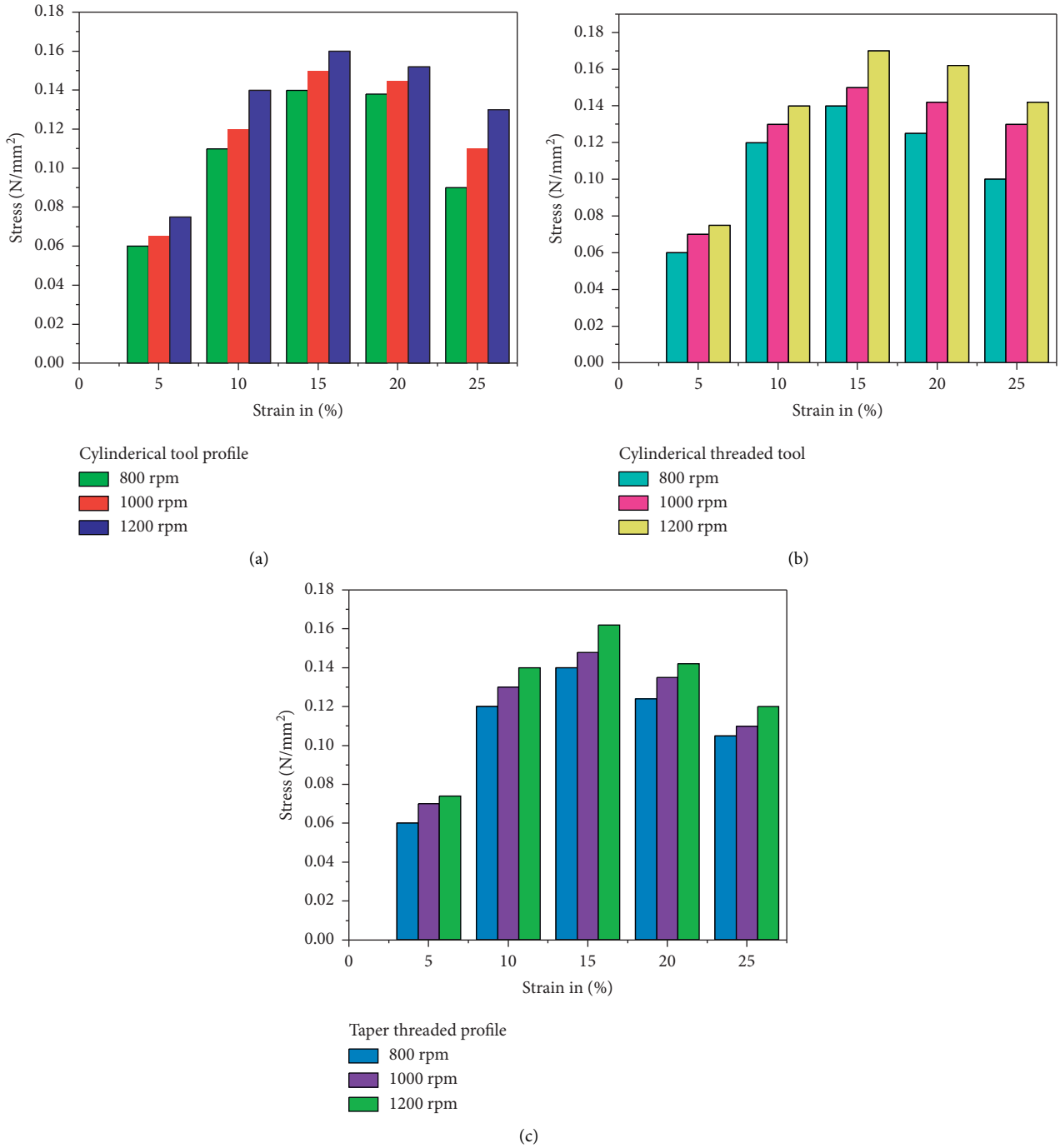

Figure 4: Tensile test: (a) cylindrical contour of the tool, (b) profile of a cylindrical threaded tool, and (c) profile of a tapered tool.

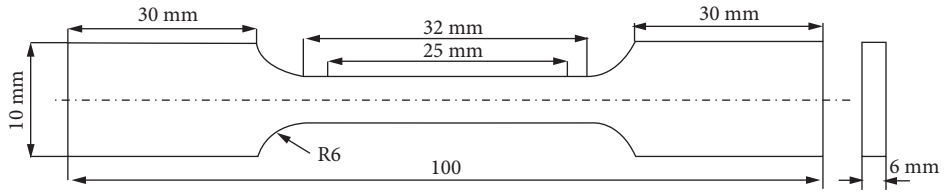

Figure 5: Dimensions of the tensile specimen (ASTM E8M-04).

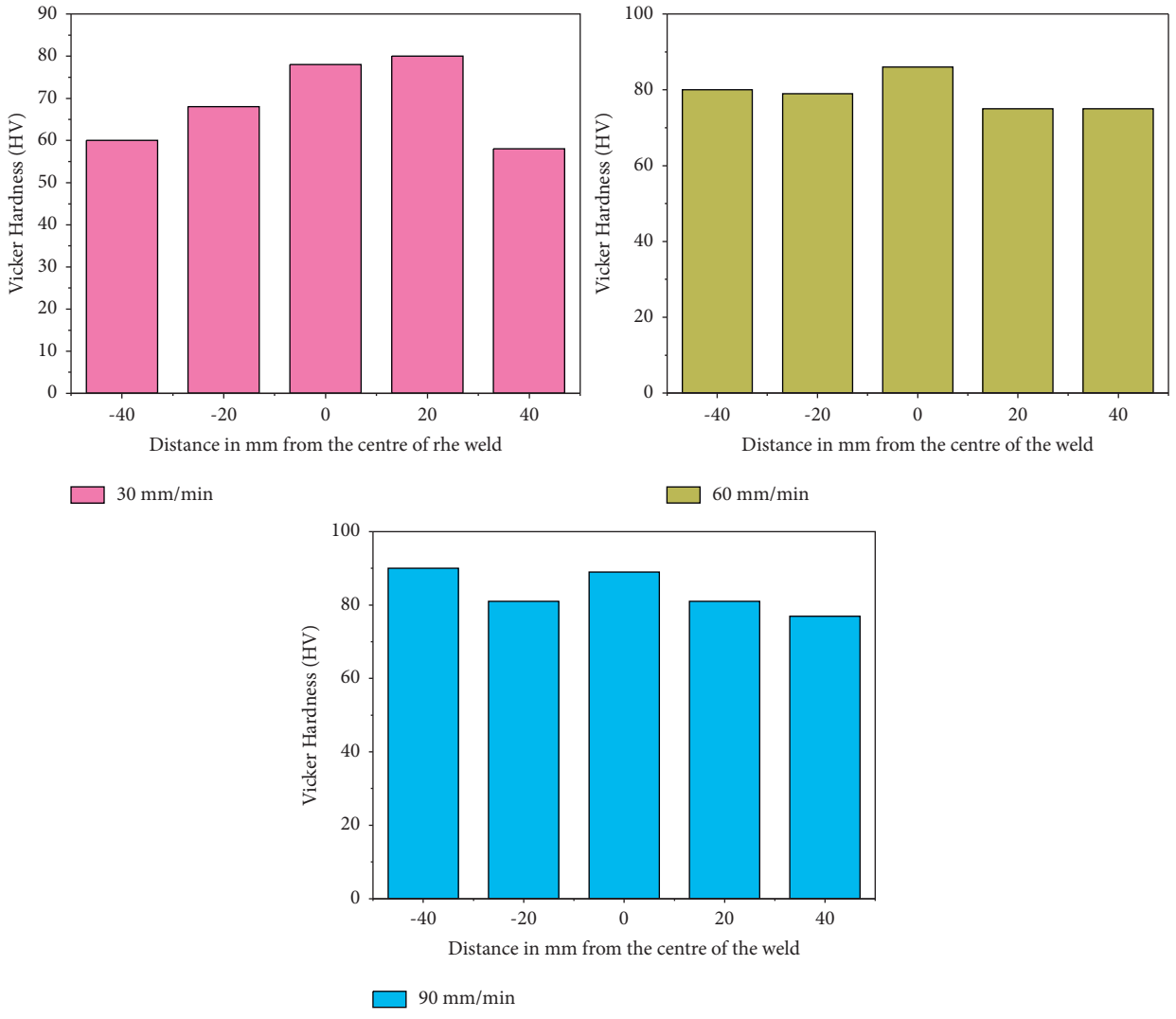

Figure 6: Vickers hardness value for the cylindrical tool.

variation region using various tool profiles. Both dissimilar alloys have their TMAZ zones located in different places. Nevertheless, the variation in hardness values has been detected at diverse locations.

4. Result and Discussion

4.1. Tensile Test. The design guidelines in ASTM standards are followed when performing tensile tests. To ensure welding consistency and testing repeatability, three separate pin profiles were used for the welded junctions. You will see the tallied test results, as well as graphs. Welded work pieces with three different profile examples offer good mechanical properties as seen in the graph of the welded area. In addition to its tensile properties, the material also displays the locations where it is broken. NZs' tool pin profiles have been evaluated on the cracked area.

As the base material's mechanical characteristics and tensile behaviour are increased, the joint welded precipitation hardening portions' tensile properties increase as well. As a result of precipitation hardening dissolving seams that have changed tensile properties, it changes grain boundaries

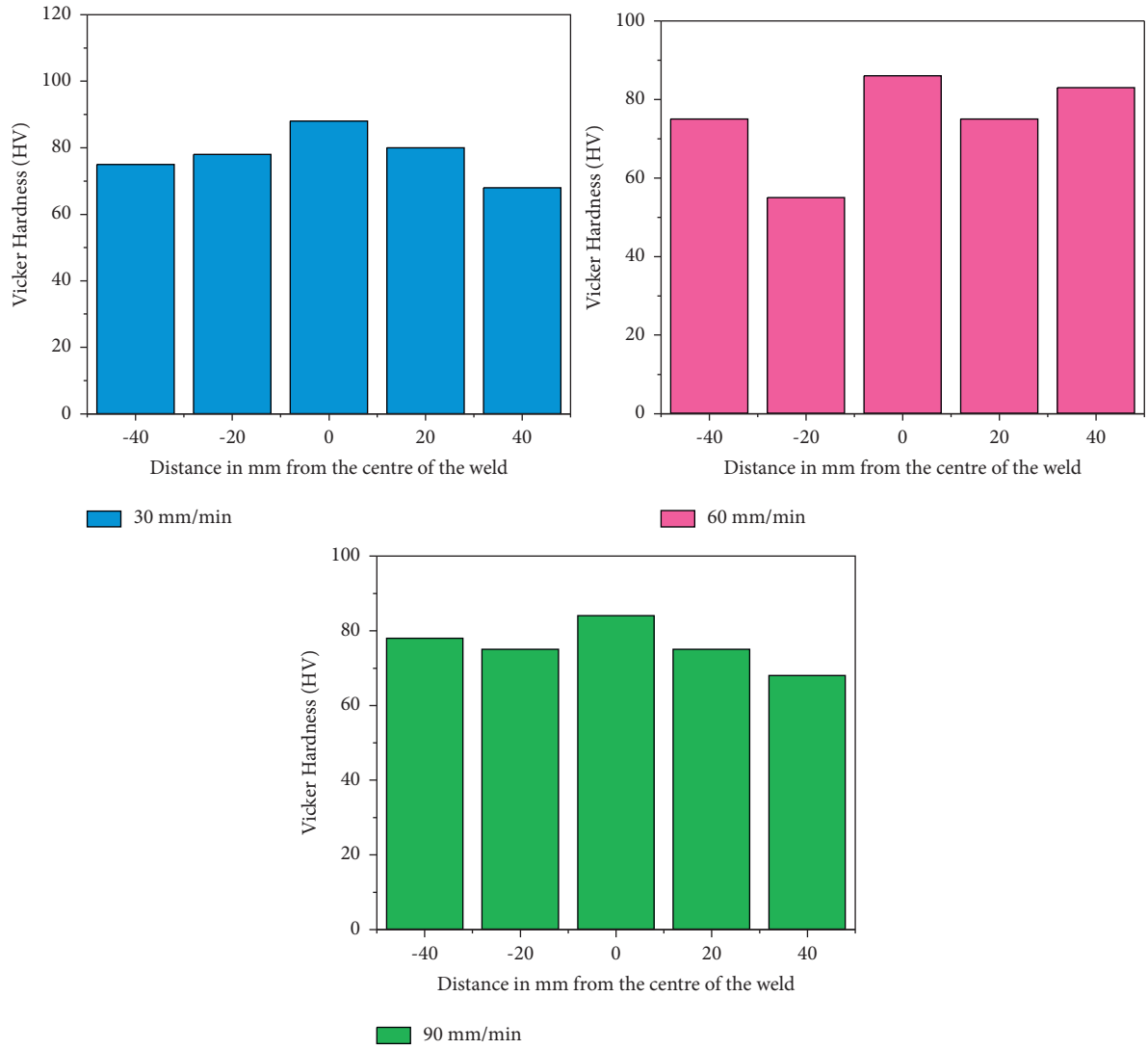

Figure 7: Vickers hardness value for the threaded cylindrical tool.

and grain orientations. All nine samples' joints have low ductility when viewed from above, ensuring the strength of the different alloys, and it is shown in Figure 4.

The specimen's dimensions are depicted in Figure 5. The speed of rotation, spindle speed, and D/d ratios with the best values were determined to be 1300 revolutions per minute, 80 millimetres per minute, and 6. When compared to the other profiles, the cylindrical threaded profile had the best result. It is responsible for 93% of the overall efficiency of the system. The cylindrical threaded tool achieved a maximum strength of 195 MPa. Welded joint tensile behaviour is studied for its impact. Because of this, welded joints have a lower strength rating than those made from other PM materials.

The fracture behaviour occurs in contrast to zones because the agitated zone or NZs are indented. The ductility of the materials was demonstrated by fracturing at a maximum stress condition. Additionally, the TMAZ of the AA 2219 and AA 7068 fractures were affected.

4.2. Hardness Measurements. The graph illustrates the hardness values for various welding speeds, transverse speeds, and ultimate strength. The NZs of hardenability were recognized as a result of their great bonded strength and high hardness values. As the advance side (AA 2219) and the retraction side (AA 7068) have raised consistently, these numbers show a decrease from the beginning. The graph values, as shown in Figures 6–8, also show that the separate zones performing to improve the welding ability of various constructions can be found. TMAZ zones have advanced sides (AA 2219) that are greater than retracted sides (AA 7068) along these values (lowest hardness zone) (minimum hardness zone). A NZ will indicate that the tensile specimen has fractured. The fine grain sizes of the different alloys are depicted as the welding direction of the agitated zone. As AA 2219 materials, it plays an essential part in the character of the mixture. The ideal settings for the taper threaded tool profile were determined to gradually increase the toughness to 92 HV: transverse rate of 60 mm/min and spindle speed of

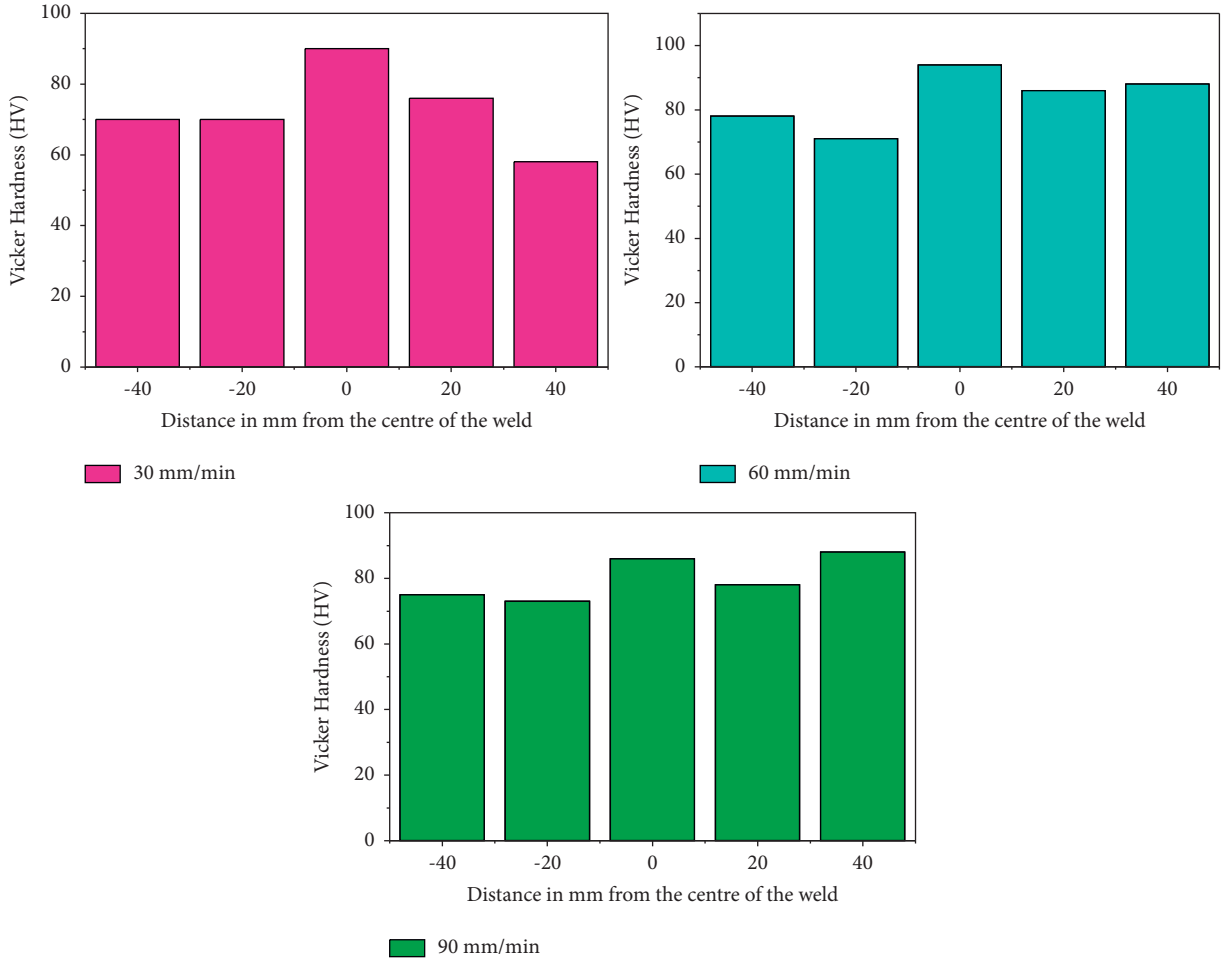

Figure 8: Vickers hardness value for the taper tool.

1000 rpm. Increase speed of rotation further and lower toughness, as with the last tool profile. When the speed is maintained at 1,300 rpm, the toughness decreases. The welded zone had the highest toughness, and mean data were derived for every test. In HAZ, the value of almost hardness increased steadily. The forward-moving side has higher hardness values than the retracting side, which has a lower value. The cylindrical tool profile has higher hardness ratings. Compared to TMAZ zones, NZs appear to have a higher value, while tensile modulus is indicative of the extent of hardness. The toughness rating of the taper threaded profile was greater.

4.2.1. Nugget Zones. The graph illustrates how the hardness values of the tools varied. It is a nonmetallic and thermomechanical influenced zone in which materials combine under a variety of weld connection process settings. The effectiveness of various optimal material flow limitations in the NZ and other recrystallization zones demonstrates the critical nature of tool profiles. There are some test components that do not have enough loading conditions to identify all of the failures. When it comes to FSW, the crystallization effect plays a critical role. It aids in regulating the high degree of softening NZs by lowering the base material's hardness from its centre line and rotational speed.

4.2.2. TMAZ Zones. It was part of the zone that was impacted by thermodynamics and relates to the NZs. The FSW process looked at how weld zones are linked together. The grain sizes control the heat response formed to the midline weld of two alloys, which have a powerful effect on the structures due to the work-hardening state. High temperatures and mechanical pressure were used to join the structure with the two different alloys, resulting in a stronger weld. Some people on the NZ border describe it as having two different alloys in it. The metal matrix has increased hardness due to the fine and homogeneous distribution of strengthening particles. HAZ is located in a very convenient place in relation to New Zealand. This operation's high humidity and temperature accelerated grain growth, which changed the direction of grain flow. On the surface of this NZ, heat and mechanical forces have been applied and have both operated. The eutectics re-emerged from the alumina crystalline phase and fragmented during the heating and chilling phases are formed due to the nugget tool's pin. This part has both the nugget's and the TMT zone's user

interfaces. TMT illustrates larger particles that were not in touch with the instrument but shifted their orientation due to plastic movement, whereas NZ illustrates small eutectic particles.

Shoulder area of the FSW-treated specimen: an advancing zone has grain flow caused by mechanical forces, and this generates heat because of frictional losses. As a result of the pin on the nugget tool spinning throughout the heating and cooling cycles, the eutectics re-emerged and fractured from the aluminium solid solution. The HAZ in the vicinity of the FSW zone has been identified. The eutectics' particle size is increasing.

This is a HAZ, but the grains have not become any bigger because the wind has shifted the direction. HAZ occurs when the eutectics' particles grow in size as a result of the growth, but the particles grow identical to that of the weld bead particles.

5. Conclusions

Good weldability and performance attributes can be produced from dissimilar alloys with FSW. For cylindrical threaded profile pins with a higher D/d ratio, this study concluded that rotational speed, transverse speed, and rotational deflection were more efficient. Cylindrical threaded tools produce maximum tensile strength, which is strong compared to other materials. Compared to the other tool profiles, the cylindrically threaded profile performs the best. The maximum strength of the joint formed with a cylindrical threaded tool rotating at 1,300 rpm and transversely moving at 80 mm/min was 195 MPa. The 110 HV value was attained by using a taper threaded cylindrical shape. Both alloys (AA2219 and AA7068) formed a bond due to the tool's behaviour (AA2219 and AA7068). Vickers hardness tests were used to determine which alloys had the best structural properties. Keller Reagent's effects were used to polish the surface more frequently while also acquiring the functional working zone's FSW. It utilizes advanced mechanical properties and character traits. It was done to determine the weld consistency, and it was done multiple times with different optimization settings. Out of the three-pin profiles, the cylinder-threaded tool has the most gain in strength.

Data Availability

The data used to support the findings of this study are included within the article. Further data or information are available from the corresponding author upon request.

Conflicts of Interest

The authors declare that there are no conflicts of interest regarding the publication of this paper.

Acknowledgments

The authors thank to Loyola-ICAM College of Engineering and Technology, Chennai, and Prince Sattam bin Abdulaziz University, Saudi Arabia, for providing technical assistance to complete this experimental work.

References

[1] K. Mariyappan, K. Praveen, S. Suresh Kumar, K. Kadambanathan, S. Rajamanickam, and R. Vignesh, "Characterization of brass/steel plates joined by friction stir welding," *International Journal of Engineering & Technology*, vol. 7, no. 3, pp. 366–368, 2018.

[2] B. V. Desai, K. P. Desai, and H. K. Raval, "The performance of tool shape on efficiency and quality of forming in incremental sheet-forming process," *International Journal of Rapid Manufacturing*, vol. 6, no. 4, pp. 215–234, 2017.

[3] T. Sathish, S. Tharmalingam, V. Mohanavel et al., "Weldability investigation and optimization of process variables for TIG-welded aluminium alloy (AA 8006)," *Advances in Materials Science and Engineering*, vol. 2021, Article ID 2816338, 17 pages, 2021.

[4] S. Murali, A. Chockalingam, S. Suresh Kumar, and M. Remanan, "Production, characterization and friction stir processing of AA6063-T6/Al3Tip in-situ composites," *International Journal of Mechanical and Production Engineering*, pp. 399–406, 2018.

[5] R. Manikandan and G. Elatharasan, "Effect of process parameters on microstructural and mechanical properties of friction stir welded dissimilar aluminium alloys AA 6061 and AA 7075," *International Journal of Rapid Manufacturing*, vol. 9, no. 1, pp. 1–15, 2020.

[6] K. Elangovan, V. Balasubramanian, and M. Valliappan, "Effect of welding speed and tool pin profile on tensile properties of friction stir welded AA6061 aluminium alloy," *International Journal of Microstructure and Materials Properties*, vol. 4, no. 4, pp. 455–475, 2009.

[7] J. Francis, T. E. Sparks, J. Ruan, and F. Liou, "Multi-axis tool path generation for surface finish machining of a rapid manufacturing process," *International Journal of Rapid Manufacturing*, vol. 4, no. 1, pp. 66–80, 2014.

[8] X. He, F. Gu, and A. Ball, "Recent development in finite element analysis of self-piercing riveted joints," *International Journal of Advanced Manufacturing Technology*, vol. 58, no. 5, pp. 643–649, 2012.

[9] X. He, "Finite element analysis of laser welding: a state of art review," *Materials and Manufacturing Processes*, vol. 27, no. 12, pp. 1354–1365, 2012.

[10] X. He, "Recent development in finite element analysis of clinched joints," *International Journal of Advanced Manufacturing Technology*, vol. 48, no. 5–8, pp. 607–612, 2010.

[11] P. Tasić, I. Hajro, D. Hodžić, and D. Dobraš, "Energy efficient welding technology: Fsw," in *Proceedings of the 11th International Conference on Accomplishments in Electrical and Mechanical Engineering and Information Technology*, Banja Luka, Bosnia and Herzegovina, May 2013.

[12] P. Xue, D. R. Ni, D. Wang, B. L. Xiao, and Z. Y. Ma, "Effect of friction stir welding parameters on the microstructure and mechanical properties of the dissimilar Al–Cu joints," *Materials Science and Engineering A*, vol. 528, no. 13–14, pp. 4683–4689, 2011.

[13] Z. Zhang, Y. L. Liu, and J. T. Chen, "Effect of shoulder size on the temperature rise and the material deformation in friction stir welding," *International Journal of Advanced Manufacturing Technology*, vol. 45, no. 9, pp. 889–895, 2009.

[14] A. Heidarzadeh, H. Khodaverdizadeh, A. Mahmoudi, and E. Nazari, "Tensile behavior of friction stir welded AA 6061-T4 aluminum alloy joints," *Materials & Design*, vol. 37, pp. 166–173, 2012.

[15] M. Jayaraman, R. Sivasubramanian, V. Balasubramanian, and A. K. Lakshminarayanan, "Application of RSM and ANN to predict the tensile strength of Friction Stir Welded A319 cast aluminium alloy," *International Journal of Manufacturing Research*, vol. 4, no. 3, pp. 306–323, 2009.

[16] M. Mehta, A. Arora, A. De, and T. DebRoy, "Tool geometry for friction stir welding-optimum shoulder diameter," *Metallurgical and Materials Transactions A*, vol. 42, no. 9, pp. 2716–2722, 2011.

[17] G. Padmanaban and V. Balasubramanian, "Selection of FSW tool pin profile, shoulder diameter and material for joining AZ31B magnesium alloy - an experimental approach," *Materials & Design*, vol. 30, no. 7, pp. 2647–2656, 2009.

[18] R. Rai, A. De, H. K. D. H. Bhadeshia, and T. DebRoy, "Review: friction stir welding tools," *Science and Technology of Welding & Joining*, vol. 16, no. 4, pp. 325–342, 2011.

[19] C. Chanakyan and S. Sivasankar, "Parametric advancement of numerical model to predict the mechanical properties of friction stir processed AA5052," *International Journal of Rapid Manufacturing*, vol. 8, no. 1–2, pp. 147–160, 2019.

[20] Z. Zhang and H. J. Liu, "Effect of pin shapes on material deformation and temperature field in friction stir welding," *Transactions of the China Welding Institute*, vol. 32, pp. 5–8, 2011.

[21] D. Zhang, N. G. Deen, and J. A. M. Kuipers, "Numerical simulation of the dynamic flow behavior in a bubble column: a study of closures for turbulence and interface forces," *Chemical Engineering Science*, vol. 61, no. 23, pp. 7593–7608, 2006.

[22] A. Arora, A. De, and T. DebRoy, "Toward optimum friction stir welding tool shoulder diameter," *Scripta Materialia*, vol. 64, no. 1, pp. 9–12, 2011.